

The Conformation of ATP within the Na,K-ATPase Nucleotide Site: A Statistically Constrained Analysis of REDOR Solid-State NMR Data**

David A. Middleton,* Eleri Hughes, and Mikael Esmann

P-type ATPases are membrane-embedded ion pumps that are present in all animal cells. ATPases utilize the energy released from adenosine triphosphate (ATP) hydrolysis to drive the vectorial transport of ions. Na,K-ATPase (NKA) contributes to the maintenance of cellular potentials by actively exchanging intracellular Na^+ for K^+ ions; this exchange is facilitated by two enzyme conformations referred to as E_1 and E_2 .^[1] When sufficient Na^+ ions are present to induce the E_1 conformation, NKA exhibits high affinity towards ATP and adenosine diphosphate (ADP). Some 50 years after the discovery of NKA, two structures of the enzyme in the absence of a nucleotide were recently determined by X-ray crystallography.^[2] The conformation of the ATP substrate in the high-affinity site is unknown.

Solid-state nuclear magnetic resonance (SSNMR) is a powerful technique for the structural analysis of organic ligands complexed with membrane-embedded receptors.^[3] Rotational-echo double resonance (REDOR) is an SSNMR method for measuring heteronuclear (e.g., ^{13}C – ^{15}N , ^{13}C – ^{31}P) dipolar couplings that encode interatomic distances.^[4] REDOR may be exploited to measure structurally diagnostic distances between carbon sites and the three phosphorus sites ($\text{P}\alpha$, $\text{P}\beta$, and $\text{P}\gamma$) of ATP when complexed with NKA. However, the quality of REDOR data is compromised by the poor sensitivity of NMR spectroscopy and the low abundance of membrane receptors. We have alleviated these difficulties by using statistical information to assist the analysis of REDOR data, and present the first experimentally derived conformation of ATP in the high-affinity nucleotide site of NKA in native membranes.

Figure 1 a shows a ^{31}P NMR spectrum of $[\text{U-}^{13}\text{C},^{15}\text{N}]\text{ATP}$ complexed with approximately 16 nmol NKA and stabilized by freeze-trapping.^[5] The equilibrium binding curves are consistent with rapid nucleotide binding to a single site, and dissociation constants are in the range of 0.2–0.5 μM and a

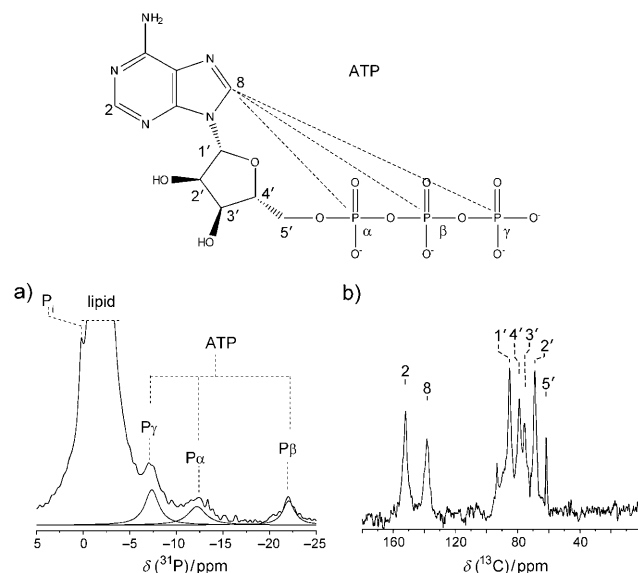


Figure 1. Structure of ATP and SSNMR spectra of $[\text{U-}^{13}\text{C},^{15}\text{N}]\text{ATP}$ complexed with NKA (at -25°C). Dotted lines on the structure of ATP denote the three C–P distances measured here. a) ^{31}P MAS spectrum of bound ATP. P_i denotes inorganic phosphate ions. Peaks are assigned according to Ref. [5]. b) ^{13}C CP-MAS spectrum of the same sample, obtained after subtraction of the background signals of the lipids and the protein. Peaks are assigned according to Ref. [13].

capacity of about 2.9 nmol mg^{-1} .^[5,6] Under these conditions, we estimate that approximately 90% of the nucleotide is bound to NKA. The procedure to form the complex prior to freeze-trapping took less than 10 min, during which less than 10 μmol ATP were hydrolyzed out of the 160 μmol present.^[6] This result is confirmed by the ^{31}P NMR spectrum, which shows signals for the three phosphate groups of ATP in approximately equal intensity. Figure 1 b shows a cross-polarization magic-angle spinning (CP-MAS) ^{13}C NMR spectrum after subtracting the background signals of the lipids and the protein. We elected to measure $\text{P}\alpha$ –C8, $\text{P}\beta$ –C8, and $\text{P}\gamma$ –C8 dipolar couplings simultaneously in a frequency-selective DANTE- $^{31}\text{P}(^{13}\text{C})$ -REDOR experiment^[7] with ^{31}P observation and dephasing selective for C8. The C8 signal is well resolved and favorable for selective inversion in the REDOR experiment. Couplings between ^{31}P and C5' or C2, which are also resolved in the spectrum, could provide additional structural restraints, but were not measured because of the lengthy data collection times involved.

REDOR dephasing (S_D) was monitored from the $\text{P}\alpha$, $\text{P}\beta$, and $\text{P}\gamma$ signal intensities at three echo times (26 days of data

[*] Dr. D. A. Middleton, Dr. E. Hughes
School of Biological Sciences, University of Liverpool
Crown Street, Liverpool L79 7ZB (UK)
E-mail: middleda@liv.ac.uk

Prof. Dr. M. Esmann
Department of Physiology and Biophysics, Aarhus University
Ole Worms Allé 6, 8000 Aarhus C (Denmark)

[**] We thank the British Heart Foundation (Grant PG/06/138) and the Aarhus University Research Foundation (F-2008-SUN-1-45) for financial support. ATP = adenosine triphosphate, REDOR = rotational-echo double resonance.

Supporting information for this article is available on the WWW under <http://dx.doi.org/10.1002/anie.201100736>.

collection). A ^{31}P MAS spectrum recorded after the REDOR experiment was virtually identical to the initial spectrum in Figure 1 a, thus confirming that ATP hydrolysis was negligible over this period. The apparently short ^{31}P echo lifetimes ($T_2 \approx 1.5$ ms, estimated from the full-echo spectra) result in large errors at the longest (4 ms) echo time even though signal accumulation was eight times longer than at the 2 ms echo time. Comparison of the S_0 values with simulated curves gives distances of (4.5 ± 0.5) Å for $\text{P}\alpha\text{-C8}$, (4.4 ± 0.4) Å for $\text{P}\beta\text{-C8}$, and a $\text{P}\gamma\text{-C8}$ distance greater than 6.0 Å (Figure 2 a). A set of

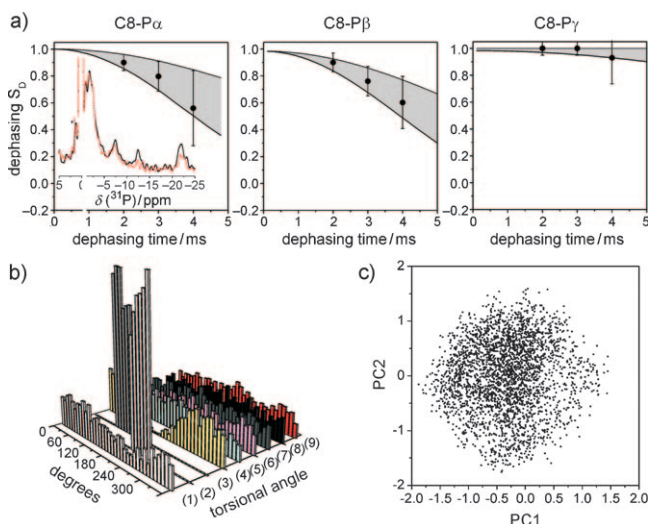


Figure 2. ^{31}P , ^{13}C -REDOR measurements for $[\text{U-}^{13}\text{C}, ^{15}\text{N}]\text{ATP}$ complexed with NKA. a) Plots of dephasing measured from the peak intensities for $\text{P}\alpha$, $\text{P}\beta$, and $\text{P}\gamma$. Errors are estimated from the level of noise. The solid lines bounding the grey regions are calculated dephasing curves corresponding to the upper and lower limits of the ^{31}P – ^{13}C distance range (see main text). The inset shows REDOR spectra at a 4 ms dephasing time (black: control, red: dephased). b) 3D histogram of torsional angle distributions (in 10° bins) consistent with the REDOR distances. c) Scores plot of the first two principal components (PC1 and PC2) calculated from the values of the nine torsional angles for each of the constrained conformers.

200 000 ATP conformations was computed stochastically, noting the values of torsional angles (1)–(9) (defined in Table 1) consistent with the three measured distances. The C8-P distances alone are poor structural restraints as very few values of (1)–(9) are excluded (Figure 2 b) and principal component analysis (PCA) of the nine angles did not identify clear patterns in the restrained conformations (Figure 2 c). This unsatisfactory outcome is a result of the few independent distances that could be measured, and is compounded by the uncertainties in the distance values.

Adenyl nucleotide ligands may generally adopt preferred conformations, which could help to strengthen the REDOR distance restraints. We analyzed coordinates for ATP, ADP, and adenosine monophosphate (AMP) ligands from 437 crystal structures of a variety of soluble proteins in the protein data bank (PDB). The nucleotide $\text{P}\alpha\text{-C8}$, $\text{P}\beta\text{-C8}$, and $\text{P}\gamma\text{-C8}$ distances measured from the PDB coordinates are distributed multimodally (Figure 3 a). Torsional angles (1)–(7) and, to a lesser extent, (8) and (9), assume correspondingly restricted

Table 1: Definition of torsional angles (1)–(9) and summary of the angular values (standard deviation in brackets) for groups A–E in Figure 4 a. The numbering system is defined in Figure 1.

Torsional angle	Value [°]				
	A	B	C	D	E
(1) C8-N9-C1'-O4'	49 (11)	49 (12)	50 (12)	50 (11)	50 (11)
(2) N9-C1'-O4'-C4'	223 (8)	224 (8)	225 (8)	224 (8)	225 (8)
(3) C1'-O4'-C4'-C5'	122 (17)	122 (17)	118 (15)	124 (15)	123 (15)
(4) O4'-C4'-C5'-O5'	297 (16)	302 (16)	307 (14)	311 (12)	310 (13)
(5) $\text{C4'-C5'-O5'-P}\alpha$	197 (24)	202 (23)	201 (24)	210 (21)	211 (21)
(6) $\text{C5'-O5'-P}\alpha\text{-O}\alpha$	106 (22)	107 (19)	119 (21)	120 (20)	126 (17)
(7) $\text{O5'-P}\alpha\text{-O}\alpha\text{-P}\beta$	43 (9)	43 (8)	152 (15)	155 (16)	164 (14)
(8) $\text{P}\alpha\text{-O}\alpha\text{-P}\beta\text{-O}\beta$	140 (19)	133 (16)	134 (16)	148 (34)	281 (20)
(9) $\text{O}\alpha\text{-P}\beta\text{-O}\beta\text{-P}\gamma$	163 (16)	82 (8)	85 (10)	151 (20)	156 (16)

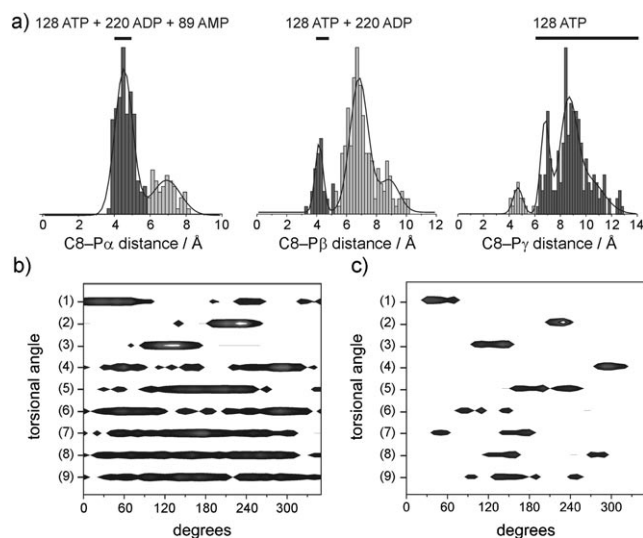


Figure 3. Conformational preferences of adenine nucleotides. a) Histograms showing the multimodal distribution of C-P distances for adenyl nucleotide ligand coordinates (numbers given) taken from the PDB. The dark-gray regions highlight the distributions which encompass the distance ranges measured by REDOR (denoted by black bars). b) Histogram (2D contour representation) of torsional angle distributions from the nucleotide structure set. Light-gray contours denote the highest frequencies. c) Histogram of torsional angle distributions for the nucleotide structures corresponding to the dark-gray regions in (a).

distributions (Figure 3 b), thus confirming that adenyl nucleotides have favored conformations. We isolated a subset of ligands for the C8-P distance distributions that encompass the REDOR distances for the ATP–NKA complex (highlighted in dark gray in Figure 3 a). The structures of the corresponding protein partners were inspected in order to ascertain whether this subset of ligands is biased toward conformations imposed by specific types of nucleotide binding domain (NBD), which may or may not be relevant to NKA. We found no common NBD for approximately 60 % of the structures, but for the ATP ligands about 20 % of NBDs were of the adenyl transferase type and around 20 % were of the tRNA synthetase type. These two latter NBD types can accommo-

date other ATP conformations that are not consistent with the REDOR data, however. We conclude that the subset of nucleotide conformations selected by NMR spectroscopy is not biased in favor of, or predictive of, a specific NBD type.

The torsional angle distributions (1)–(9) for the subset (Figure 3c) are much narrower than seen in the statistically unconstrained REDOR analysis (Figure 2b), thus indicating that the distance restraints are considerably stronger when conformational preferences are applied. A fresh set of 200 000 ATP conformations was generated by imposing the torsional angle ranges in Figure 3c. Each conformation that satisfies all three REDOR distance restraints is represented as a point on the PC scores plot in Figure 4a. The points now cluster into

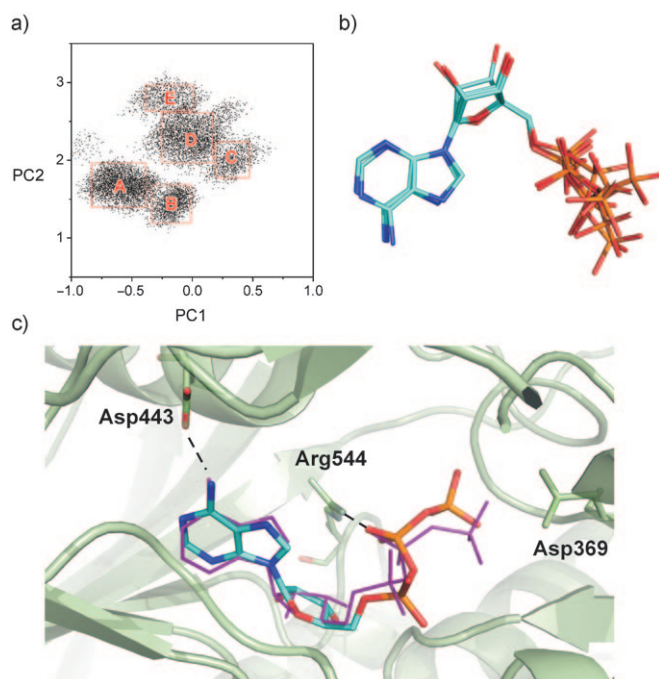


Figure 4. Constrained conformational analysis for [U-¹³C,¹⁵N]ATP complexed with NKA. a) PC scores plot of ATP conformers generated stochastically by varying angles (1)–(9) within the limits imposed by the histogram in Figure 3c. b) Superposition of five representative ATP structures from each cluster A–E. c) Homology model of the NKA nucleotide binding site, based on a structure of SERCA.^[8] The model incorporates AMPPCP (magenta) at its position within the SERCA structure with a representative ATP structure aligned to it. Arg = arginine; Asp = aspartic acid.

five distinct groups (A–E) that are characterized by the torsional angle combinations in Table 1. Representative structures from each group overlaid in Figure 4b show high similarity in the region between C8 and P α .

We modeled the NKA nucleotide site based on the structure of the sarco(endo)plasmic reticulum Ca²⁺-ATPase (SERCA) with a bound ATP analogue (AMPPCP).^[8] All ATP structures fit within the nucleotide site, but the representative structure from group A has the geometry that is most favorable for placing the γ -phosphate close to the NKA phosphorylation site Asp369 and the adenyl ring close to Asp443. Mutation of Asp369 to Asn or Ala—removing one

net negative charge on the protein—leads to a 40-fold increase in affinity for ATP because of a severely lowered electrostatic repulsion between the negative charge on the γ -phosphate and the mutated residue.^[9] In addition, mutation of Asp443 affects the Mg²⁺ binding to ATP^[10] and the negative charge on Arg544 has been shown to be important for ATP binding.^[11] In our model, Asp443 hydrogen bonds with N5 of ATP, and Arg544 is capable of an ionic interaction with the ATP β -phosphate. The results of these mutations and the remarkable conformational similarity of ATP and AMPPCP thus corroborate our model.

In conclusion, REDOR structural analysis of membrane protein ligands may be improved dramatically by considering ligand conformational preferences. A similar approach could be applied to molecules such as amino acids and saccharides, which are well-represented as soluble protein ligands in the PDB but which are structurally poorly represented as membrane protein ligands.

Experimental Section

NKA membranes from pig kidney and the [U-¹³C,¹⁵N]ATP–NKA complex were prepared as previously described.^[5,6] NMR experiments were performed at –25°C using a Bruker Avance 400 spectrometer at a magnetic field of 9.3 T. Samples were spun at an MAS rate of 10 kHz in a 4 mm zirconium rotor. The pulse sequence described in Ref. [7] was adapted for DANTE-³¹P,¹³C-REDOR experiments. The numbers of scans at each dephasing time were 80 K at 2 ms, 320 K at 3 ms, and 640 K at 4 ms. Dephasing curves were simulated in the SIMPSON^[12] environment for a four-spin system of P α , P β , P γ , and C8, taking into account the ³¹P–³¹P *J*-coupling and dipolar coupling constant. Further experimental details are given in the Supporting Information.

Received: January 28, 2011

Revised: May 5, 2011

Published online: June 10, 2011

Keywords: adenosine triphosphate · conformation analysis · NMR spectroscopy · nucleotide ligands · torsional angles

- [1] P. L. Jørgensen, S. J. D. Karlsh, A. B. Maunsbach, *Na,K-ATPase and Related Cation Pumps* **2003**, 986, 1.
- [2] a) J. P. Morth, B. P. Pedersen, M. S. Toustrup-Jensen, T. L. M. Sørensen, J. Petersen, J. P. Andersen, B. Vilsen, P. Nissen, *Nature* **2007**, 450, 1043; b) T. Shinoda, H. Ogawa, F. Cornelius, C. Toyoshima, *Nature* **2009**, 459, 446.
- [3] a) P. T. F. Williamson, A. Verhoeven, K. W. Miller, B. H. Meier, A. Watts, *Proc. Natl. Acad. Sci. USA* **2007**, 104, 18031; b) A. Watts, *Nat. Rev. Drug Discovery* **2005**, 4, 555; c) S. Luca, J. F. White, A. K. Sohal, D. V. Filippov, J. H. van Boom, R. Grishammer, M. Baldus, *Proc. Natl. Acad. Sci. USA* **2003**, 100, 10706; d) J. J. Lopez, A. K. Shukla, C. Reinhart, H. Schwalbe, H. Michel, C. Glaubitz, *Angew. Chem.* **2008**, 120, 1692; *Angew. Chem. Int. Ed.* **2008**, 47, 1668.
- [4] J. A. Watts, A. Watts, D. A. Middleton, *J. Biol. Chem.* **2001**, 276, 43197.
- [5] D. A. Middleton, E. Hughes, N. U. Fedosova, M. Esmann, *ChemBioChem* **2009**, 10, 1789.
- [6] N. U. Fedosova, P. Champeil, M. Esmann, *Biochemistry* **2002**, 41, 1267.

- [7] L. B. Andreas, A. K. Mehta, M. A. Mehta, *J. Am. Chem. Soc.* **2007**, *129*, 15233.
 - [8] C. Toyoshima, T. Mizutani, *Nature* **2004**, *430*, 529.
 - [9] P. A. Pedersen, J. H. Rasmussen, P. L. Jørgensen, *Biochemistry* **1996**, *35*, 16085.
 - [10] D. Strugatsky, K. E. Gottschalk, R. Goldshleger, S. J. D. Karlsh, *Biochemistry* **2005**, *44*, 15961.
 - [11] M. D. Jacobsen, P. A. Pedersen, P. L. Jørgensen, *Biochemistry* **2002**, *41*, 1451.
 - [12] M. Bak, J. T. Rasmussen, N. C. Nielsen, *J. Magn. Reson.* **2000**, *147*, 296.
 - [13] U. A. Hellmich, W. Haase, S. Velamakanni, H. W. van Veen, C. Glaubitz, *FEBS Lett.* **2008**, *582*, 3557.
-